RESEARCH ARTICLE

New insight into stratification of anaerobic methanotrophs in cold seep sediments

Irene Roalkvam[1], Steffen Leth Jørgensen[1], Yifeng Chen[2], Runar Stokke[1], Håkon Dahle[1], William Peter Hocking[1], Anders Lanzén[1], Haflidi Haflidason[3] & Ida Helene Steen[1]

[1]Department of Biology, Centre for Geobiology, University of Bergen, Norway; [2]Guangzhou Institute of Geochemistry, Chinese Academy of Sciences, China; and [3]Department of Earth Science, Marine Geology and Geophysics, University of Bergen, Norway

Correspondence: Ida Helene Steen, Department of Biology, Centre for Geobiology, University of Bergen, PO Box 7800, N-5020 Bergen, Norway. Tel.: +47 55 58 83 75; fax: +47 55 58 37 07; e-mail: ida.steen@bio.uib.no

Received 7 December 2010; revised 16 May 2011; accepted 2 June 2011.

DOI:10.1111/j.1574-6941.2011.01153.x

Editor: Alfons Stams

Keywords
ANME-1; stratification; pyrosequencing.

Abstract

Methane seepages typically harbor communities of anaerobic methane oxidizers (ANME); however, knowledge about fine-scale vertical variation of ANME in response to geochemical gradients is limited. We investigated microbial communities in sediments below a white microbial mat in the G11 pockmark at Nyegga by 16S rRNA gene tag pyrosequencing and real-time quantitative PCR. A vertical stratification of dominating ANME communities was observed at 4 cmbsf (cm below seafloor) and below in the following order: ANME-2a/b, ANME-1 and ANME-2c. The ANME-1 community was most numerous and comprised single or chains of cells with typical rectangular morphology, accounting up to 89.2% of the retrieved 16S rRNA gene sequences. Detection rates for sulfate-reducing *Deltaproteobacteria* possibly involved in anaerobic oxidation of methane were low throughout the core. However, a correlation in the abundance of Candidate division JS-1 with ANME-2 was observed, indicating involvement in metabolisms occurring in ANME-2-dominated horizons. The white microbial mat and shallow sediments were dominated by organisms affiliated with *Sulfurovum* (*Epsilonproteobacteria*) and *Methylococcales* (*Gammaproteobacteria*), suggesting that aerobic oxidation of sulfur and methane is taking place. In intermediate horizons, typical microbial groups associated with methane seeps were recovered. The data are discussed with respect to co-occurring microbial assemblages and interspecies interactions.

Introduction

At the continental margins large amounts of methane are stored in the subsurface sediments as crystalline methane hydrates, dissolved in pore water, and as free gas (Kvenvolden *et al.*, 1993). Despite the large flux of methane in the sediment, as much as 90% of the biogenic methane is instantly consumed during anaerobic oxidation of methane (AOM) (Knittel & Boetius, 2009), hence restricting the diffusion of this potent greenhouse gas into the atmosphere. AOM is suggested to be mediated through syntrophic consortia of methanotrophic archaea [anaerobic methane oxidizers (ANME)] together with sulfate-reducing bacterial (SRB) partners. The process is catalyzed according to the following overall reaction (Nauhaus *et al.*, 2002):

$$CH_4 + SO_4^{2-} \rightarrow HCO_3^- + HS^- + H_2O \quad (1)$$

The ANME clades (ANME-1, -2 and -3) are phylogenetically affiliated with the methanogens, and form three distinct clusters related to the orders *Methanosarcinales* and *Methanomicrobiales* (Knittel & Boetius, 2009). ANME are often observed in consortia with SRB, and theories of ANME being dependent on a bacterial partner to compensate for its missing capacity for sulfate reduction were suggested early on (Hoehler *et al.*, 1994). In ANME-1 and ANME-2, the partner is typically from the *Desulfosarcina/Desulfococcus* group (Knittel *et al.*, 2005; Schreiber *et al.*, 2010), while ANME-3 is affiliated with sulfate reducers within the *Desulfobulbus* group (Niemann *et al.*, 2006; Lösekann *et al.*, 2007). However, observations of 'free-living ANME' cells, in particular ANME-1 (Knittel *et al.*, 2005), indicate that ANME mediate AOM with sulfate without a bacterial partner, challenging the universality of the syntrophic hypothesis. The major habitats of ANME clades are

methane-enriched environments, and consequently these methanotrophs are found worldwide, in for example cold seeps and mud volcanoes (Lanoil *et al.*, 2001; Orphan *et al.*, 2001; Knittel *et al.*, 2005; Lösekann *et al.*, 2007). In cold seep ecosystems, where methane is present just below the seawater-sediment interface, the ANME populations can reach a level of $> 10^{10}$ cells cm^{-3}, whereas in deeper subsurface sulfate methane transition zone the cell number decreases to as few as $< 10^{6}$ cells cm^{-3} (Orphan *et al.*, 2001). The upper layers of cold seep ecosystems are primarily dominated by ANME-2 and ANME-3 (Knittel & Boetius, 2009); however, two seep systems, in the Gulf of Mexico (Lloyd *et al.*, 2006, 2010) and microbial mats from the Black Sea (Knittel *et al.*, 2005), are known to be dominated by members of the ANME-1 clade. Aiming to provide insight into how geochemical gradients constrain the diversity, abundance and stratification of ANME clades in cold seep sediments, a sediment core sampled in a pingo-structure inside the G11 pockmark at Nyegga, the mid-Norwegian margin, was analyzed by 16S rRNA gene tag-encoded FLX pyrosequencing and real-time quantitative PCR (qPCR). The G11 pockmark is one of the most active and best described pockmarks in Nyegga, located at a water depth of ~740 m and characterized by a large number of pockmarks and fluid seepage structures (Hovland *et al.*, 2005; Hjelstuen *et al.*, 2010; Ivanov *et al.*, 2010; Reiche *et al.*, 2011). Our approach provided fine scale taxonomic information, and in combination with extensive sampling, we revealed a dynamic change in community structure with depth, influenced by the geochemical gradients in the sediment. The data are discussed with respect to vertical variation in dominating ANME-clades and their co-occurring microbial assemblages.

Materials and methods

Site description and sampling

Push cores for detailed microbial diversity studies were retrieved from the Nyegga area (64°39.788′N; 05°17.317′E), located on the upper mid-Norwegian continental slope, during August of 2008. The core GS08-155-29ROV used in this study was taken from an active pingo-structure within pockmark G11 at 746 m of water depth (Supporting Information, Fig. S1a). Tabular methane hydrates are present in sediments below 0.75 m inside pockmark G11 (Chen *et al.*, 2010). Upward-migrating methane fluids are spatially variable in the pockmark, with methane fluxes ranging from below detection limit outside the G11 to 0.30–0.54 mol m^{-2} $year^{-1}$ inside the pockmark, with exception of the center area (Chen *et al.*, 2010).

The video facilities on the ROV *Bathysaurus* were utilized to find and localize precisely the core site within a white microbial mat in the central 'hot spot' area of the pingo-structure. The Argus *Bathysaurus* ROV system applied on the research vessel *G.O.Sars* was used to retrieve the 22-cm-long push core, including a white microbial mat in the seawater-sediment interface (Fig. S1b). The ambient seawater temperature measured during sampling was $-0.6\,^{\circ}C$.

Immediately after retrieval, the push core was sectioned aseptically into 1-cm layers down to 10 cmbsf (cm below seafloor) and thereafter into 2-cm layers. From the center of each sediment layer, four sediment subsamples were taken for DNA extraction using sterile 1-mL tip cut plastic syringes, snap-frozen in liquid N_2 and stored at $-80\,^{\circ}C$. One half of the sediment sample was used for separation of sediment and pore water. The remaining bulk sediments were stored at $-80\,^{\circ}C$.

Geochemical characterization

Pore waters from five different horizons (3, 7, 11, 15 and 19 cmbsf) were obtained by centrifuging the sediment subsamples at 9000 ***g*** for 20 min at 4 °C, followed by a filtration of the supernatant through 0.2-μm membrane filters. In addition, bottom seawater was collected from 3 cm above the sediment surface. Sample aliquots were preserved in glass vials and kept cool until they were used in geochemical analyses.

The dissolved sulfate (SO_4^{2-}) concentrations were determined using a Dionex DX-120 ion chromatograph, as described by Chen *et al.* (2010). The total dissolved hydrogen sulfide (ΣH_2S) in pore water was quantitatively preserved by precipitation as ZnS using 20% zinc acetate solution, and was determined by the methylene blue method of Cline (1969) using a Thermo GENESYS 10 UV spectrophotometer. The dissolved inorganic carbon (DIC) and its stable carbon isotopes ($\delta^{13}C_{DIC}$) were determined at the stable isotope laboratory at Oregon State University, using continuous flow technology (Chen *et al.*, 2010).

DNA extraction and 16S rRNA gene amplicon sequencing

Total genomic DNA was extracted from ~0.5 g of sediment from each subsample throughout the core, using FastDNA Spin kit for soil and the FastPrep®-24 Instrument (MP Biomedicals, Santa Ana, CA) according to the protocol supplied with the kit. The DNA was eluted in 50–60 μL DNase/Pyrogen-Free Water supplied with the kit, and the concentration was determined by $A_{260\,nm}/A_{280\,nm}$ ratio measurements using a Cary 300 Bio UV–Vis Spectrophotometer (Varian Inc., Palo Alto, CA). Total genomic DNA from subsamples at 0–1, 2–3, 4–5, 6–7, 9–10, 14–16 and 20–22 cmbsf were applied in a two step PCR before the 454-amplicon sequencing. In the first PCR the V5–V8 region of the 16S rRNA gene was amplified using the universal primers

Un787f (5′-ATTAGATACCCNGGTAG) (Roesch *et al.*, 2007) and Un1392r (5′-ACGGGCGGTGWGTRC) modified from (Lane *et al.*, 1985).

The template DNA concentrations were titrated in order to achieve optimum PCR conditions (1–10 ng DNA μL^{-1}). Each reaction contained 1 × HotStar Taq® Master Mix kit (Qiagen, Hilden, Germany), 1 μM of each primer and 1 μL template. The thermal cycling program was 95 °C for 15 min and then 25–30 cycles of 45 s at 95 °C, 45 s at 53 °C and 1 min at 72 °C, followed by 72 °C for 7 min and cooling to 4 °C. Each sample was amplified in triplicate, and PCR products were pooled before purification with MinElute® PCR purification kit (Qiagen). The resulting DNA concentrations ranged from 0.98 to 5.3 ng μL^{-1}, measured by SYBR-Green quantification (modified from Zipper *et al.*, 2003). Briefly, duplicate samples were measured in 10-fold dilution, each reaction contained 5 μL sample and 20 μL 5 × SYBR-Green I nucleic acid gel stain (Invitrogen, Eugene, OR). The samples were incubated in Step One Plus real-time PCR system (Applied Biosystems Inc., Foster City, CA) instrument for 15 min at 22 °C, followed by a plate read. A duplicate dilution series of genomic *Escherichia coli* DNA (DNA sodium salt from *E. coli* strain B, Sigma-Aldrich Inc., St. Louis, MO) was used to generate the standard curve.

In the second PCR, the primers were modified according to specifications in Lib-L chemistry corresponding to the unidirectional 454-pyrosequencing applied in this study. In the forward primer Un787f the GS FLX Titanium Primer A sequence and a specific MID sequence of 10 bp for each sample was included. The reverse primer Un1392r had the GS FLX Titanium Primer B sequence included. The second PCR contained 1 × HotStar Taq® Master Mix kit, 0.8 μM of each primer and 10 μL template from the first PCR, in 25 μL reactions. The PCR was performed as described above, using five cycles.

Excess primers were removed using Amicon Ultra 50K centrifugation filter units (Millipore, Carrigtwohill, Ireland). Briefly, two centrifugation steps (14 000 ***g***, for 10 and 25 min, respectively) and Tris-HCl EDTA (TE) buffer (pH = 8) (500 μL in total) were applied. The concentrations of the PCR products were determined to range from 5.5 to 11.9 ng μL^{-1} by SYBR-Green quantification. All samples were pooled in a 1 : 1 ratio, comprising 35 ng DNA each in the final suspension. To ensure complete removal of excess primers and other impurities, a final purification was performed using Agencourt AMPure Beads (Beckman Coulter Genomics) according to the protocol supplied with the kit.

Sequencing of the 16S rRNA gene amplicons were performed on a Roche/454 GS-FLX system following the guidelines for Titanium amplicon sequencing. The sequencing service was provided by the Norwegian High-Throughput Sequencing Centre.

Filtering and removal of noise and chimeras from 16S rRNA gene amplicon sequences

Quality filtering and noise removal of pyrosequencing reads of 16S rRNA gene amplicons was carried out using AMPLICONNOISE (version 1.1) (Quince *et al.*, 2011). In summary, this method includes four steps: filtering, flowgram clustering, sequence-clustering and chimera removal. In the filtering step, reads with fewer flows than 360 or with a noisy signal (flow intensity 0.5–0.7) before this position were removed, in addition to all reads not matching the barcode and primer sequences. In the sequence-clustering step, reads were truncated at 400 bp. Barcode and primer sequences were removed before further analysis such as taxonomic classification and linkage clustering.

Taxonomic classification

All filtered, denoised and chimera-filtered sequences were aligned to a reference database prepared from Silva SSURef release 100 (Lanzén *et al.*, 2011) using BLASTN (default parameters) as implemented in the NCBI standalone BLAST suite. All sequences with a bit-score above 150 to any database reference sequence were classified as SSU rRNA. The BLAST result was analyzed using MEGAN version 3.7 (Huson *et al.*, 2007) in order to assign each sequence to a taxon in the modified Silva Taxonomy described above. To this end, MEGAN uses a lowest common ancestor (LCA) algorithm for which we used a minimum absolute cut-off of 150 bits and the default settings for relative cut-off. Thus, all sequences matching a reference sequence above the threshold were assigned to the node that represents their LCA of the 10% range of the best BLASTN bitscore in the taxonomy. MEGAN assignments were then exported and weighed according to its cluster's copy number. Abundance counts of each taxon at different ranks were calculated using these weighed assignments.

The raw sff-files of 16S tag-encoded amplicons from all subsamples in core 29ROV from Nyegga have been submitted to the Sequence Read Archive under the accession number SRA026733.1.

Real-time qPCR

Total genomic DNA from all subsamples was used as templates in real-time q-PCR to enumerate 16S rRNA genes from both Archaea and Bacteria. The DNA template concentration used in the PCR was 1 ng per 20 μL reaction, in duplicates. Each reaction contained 1 × Power SYBR Green PCR Master Mix (Applied Biosystems, Warrington, UK), 1 mM of each primer and 1 μL template. Genomic DNA from *Archaeoglobus fulgidus* and *E. coli* were used as negative controls during quantification of Bacteria and Archaea, respectively.

For quantification of 16S rRNA genes of bacterial origin, the primers B338f (5′-ACTCCTACGGGAGGCAGC) (Amann *et al.*, 1995) and B518r (5′-ATTACCGCGGCTGCTGG) (Muyzer *et al.*, 1993) were used. The PCR was performed using a Step One Plus real-time PCR system (Applied Biosystems Inc., Foster City, CA) with 40 cycles of the thermal program as described by Einen *et al.* (2008).

A purified PCR product obtained by amplification of the 16S rRNA gene from *E. coli* was used in a 10-fold dilution series to generate the quantification standard curve. Briefly, the PCR product was obtained using the 16S rRNA gene-specific primers B8f (5′-AGAGTTTGATCCTGGCTCAG) (Edwards *et al.*, 1989) and Un1492r (5′-GGTTACCTTGT TACGACTT) (Lane, 1991) in a conventional PCR with genomic *E. coli* DNA as template. The PCR product was quantified by $A_{260\,nm}/A_{280\,nm}$ ratio measurement, and the concentration was used to calculate 16S rRNA gene copies μL^{-1} as described by Whelan *et al.* (2003). The standard curve was applied as duplicates, ranging from 1.38×10^2 to 1.38×10^7 16S rRNA gene copies μL^{-1}. The R^2 value for the standard curve was 0.99 and the slope value was -3.49, estimating a PCR amplification efficiency of 93.43%.

Archaeal 16S rRNA genes were quantified using the primers Un519f (5′-TTACCGCGGCKGCTG) (Ovreas *et al.*, 1997) and A907r (5′-CCGTCAATTCCTTTRAGTTT) modified from (Muyzer *et al.*, 1995; S.L. Jorgensen, unpublished data). Quantification standard curve consisted of a dilution series of linearized fosmid 54d9 (Treusch *et al.*, 2005) with a copy number of archaeal 16S rRNA genes between 14.8 and 1.48×10^7 copies μL^{-1}. The R^2 value for the standard curve was 0.99 and the slope value was -3.34, giving an estimated PCR amplification efficiency of 99.25%.

Total cell number [4′,6′-diamidino-2-phenylindole (DAPI)] and FISH

Samples of approximately 1 g in 15 mL sterile seawater were homogenized in dispersing tubes (DT-20, IKA-Werke, Staufen, Germany) for 30 s at 3000 r.p.m. The homogenate was diluted to 50 mL in sterile seawater, centrifuged at 1000 ***g***, 15 min, 4 °C. Cells in the supernatant were fixed by adding formaldehyde to a final concentration of 1% and cells were stained for quantification using DAPI staining. When prepared for FISH, the cells were fixed with a 2% final concentration of paraformaldehyde, transferred to a polycarbonate membrane filter (0.2 µm pore size, Whatman, Schleider & Schuell, UK) and stored at -20 °C until used.

FISH was performed on filters with fluorescently labeled oligonucleotides (Glöckner *et al.*, 1996; Ronimus *et al.*, 1997) and DAPI (Morikawa & Yanagida, 1981). Alexa-488-labeled EUB338 I–III (Daims *et al.*, 1999), NON338 (Christensen *et al.*, 1999) and Atto-590 labeled ANME1-350 (Boetius *et al.*, 2000) were used in addition to Cy-3 double-labeled (Stoecker *et al.*, 2010) ARC917 (Loy *et al.*, 2002). Hybridizations were performed in 35% formamide for the probes ARCH917 and EUB338, while 40% formamide was used for the ANME1-350 and EUB338 probes. Positive control for the bacterial probe was fixed cells of *E. coli*, and for the archaeal probe fixed cells of *A. sulfaticallidus* (Steinsbu *et al.*, 2010). Stained slides were immersed in Immersol 518F (Zeiss) and evaluated in Zeiss Axio Imager Z1 microscope (Carl Zeiss), equipped with illumination system HXP-120 and filters for Cy3 and GFP, and Colibri with filterset 62HE (BFP+GFP+HcRed).

Results and discussion

Geochemistry

Bottom seawater had a sulfate concentration of 27.5 mM, which is lower than the typical seawater value. The DIC concentration of 2.5 mM was similar to the regional value of 2.3 mM, although the $\delta^{13}C_{DIC}$ value of -3.9‰ PDB (Pee Dee Belemnite) was much depleted in ^{13}C compared with the regional value of 0 ± 0.5‰ PDB (Chen *et al.*, 2010). Just below the seafloor surface, the pore water profiles showed a distinct pattern, where the concentration of SO_4^{2-} decreased from 16 mM at 3 cmbsf to 7.1 mM at 19 cmbsf, while the ΣH_2S concentration increased accordingly from 2.7 to 5.8 mM. Decrease of sulfate showed a strong correlation ($R^2 = 0.92$) with increase in hydrogen sulfide, indicating that hydrogen sulfide is produced during sulfate reduction (Fig. 1a). However, gas loss during sampling due to decreasing pressure apparently influenced the sulfide measurements, and sulfide concentrations should therefore be considered as minimum values.

The DIC concentration increased with depth, from 2.5 mM at the surface to 20.4 mM at 19 cmbsf. This was consistent with increasing concentrations of sulfide, possibly generated during AOM in deeper horizons. In addition, the $\delta^{13}C_{DIC}$ values of pore waters were distinctly depleted in ^{13}C, ranging from -47.1‰ to -49.0‰ PDB, which shows that DIC is derived from anaerobic oxidation of isotopically light methane by microorganisms (Reeburgh, 2007).

Abundance and taxonomy of bacterial and archaeal groups

454-pyrosequencing of 16S rRNA gene tag-encoded PCR amplicons was used to study the distribution of taxa within seven depth horizons in core 29ROV. Amplicon libraries comprising 922–18652 reads with an average read length of 230 bp (excluding primer sequence and barcode) were obtained after removal of poor-quality and chimeric sequences, excluding 14.7–22.6% of the reads from the

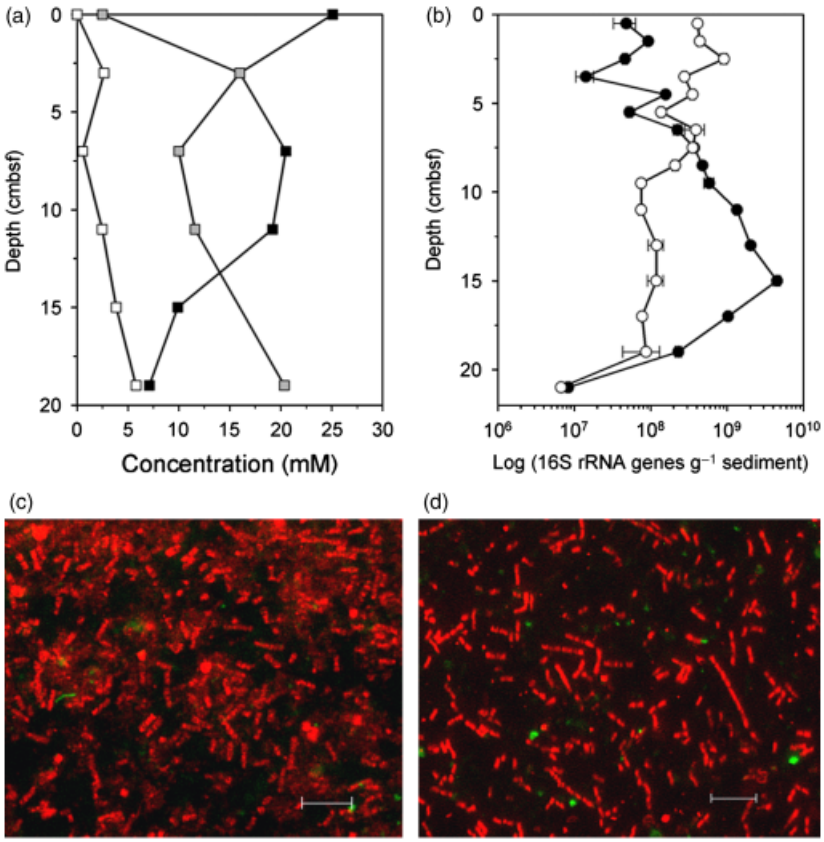

Fig. 1. Geochemical characterization, real-time qPCR and epifluorescence micrographs from core 29ROV. Sediment profile of hydrogen sulfide concentrations (□), sulfate concentrations (■) and concentration of DIC (■) (a). Enumeration of 16S rRNA genes g^{-1} sediment for Archaea (●) and Bacteria (○) using real-time qPCR (b). The error bars in (b) represent the SD calculated from the C_t values of parallel samples. The microbial community at 14–16 cmbsf visualized by FISH (c and d). Archaeal cells, shown in red, were targeted with probe ARC917 and bacterial cells were stained with EUB338 I-III, shown in green (c). ANME-1 was stained with the specific probe ANME1-350, shown in red, while probe EUB338 I-III was used for Bacteria, shown in green (d).Scale bar = 5 μm.

original dataset (Table S1). The majority of the reads were successfully taxonomically classified, with 99% classified to phylum level, 87% to class level and 77% to order level or better. However, only 46% of reads could be classified to family level and a meager 1.4% to genus level (Appendix S1). This is mainly caused by the samples being dominated by taxa that are not well described below phylum and class level, and uncultivated groups within *Thaumarchaeota*, Candidate divisions and *Planctomycetes* among others. In addition, the use of primer based PCR in the preparation of the amplicon libraries introduces a potential bias that could lead to incomplete detection of specific taxa and likewise distort their relative abundance. This should be taken into consideration when evaluating the data.

The top 8 cm of the sediment were dominated by Bacteria, while Archaea gradually increased in abundance at greater depths as revealed by taxonomic classification of the noise-filtered amplicon sequences (Fig. 2). This observation was supported by real-time qPCR of Archaea and Bacteria, separately (Fig. 1b).

The most dominating taxon in shallow horizons between sediment surface and 3 cmbsf were *Gammaproteobacteria*, constituting between 35.1% and 32.7% of the reads, of which the majority was affiliated with the order *Methylococcales* (Fig. 2b). The *Methylococcales* was also found in deeper horizons, but the abundance decreased significantly below 2–3 cmbsf (Fig. 3). In a study by Chen *et al.* (2010), the methane fluxes of 0.3–0.54 mol m^{-2} year^{-1} in G11 pockmark were measured (Chen *et al.*, 2010). Due to the high methane flux within the active pingo-structures, sufficient methane apparently reaches the oxic surface sediments to support the population of aerobic methanotrophs. The high abundance of *Methylococcales* (Fig. 2b) may also influence the observed $\delta^{13}C_{DIC}$ values of pore waters (Fig. 1a) as the metabolically produced CO_2, in addition to the degradation of dead methanotrophs, may be isotopically light. Unique sequences within the *Methylococcales* were extracted from MEGAN and used in a BLASTN search on the NCBI server. This revealed that the sequences were between 97% and 100% similar to published sequences found in similar environments, such as mud volcanoes in the East Mediterranean Sea or on the Barents Sea margin (Lösekann *et al.*, 2007; Pachiadaki *et al.*, 2010), cold seeps in Sagami Bay and Northern North Sea (Fang *et al.*, 2006; Wegener *et al.*, 2008) and hydrothermal vent systems on the Mid-Atlantic Ridge (Brazelton *et al.*, 2006; Hugler *et al.*, 2010).

In cold seep habitats, sulfur-oxidizing bacteria are often present at the seawater-sediment interface, being fueled by

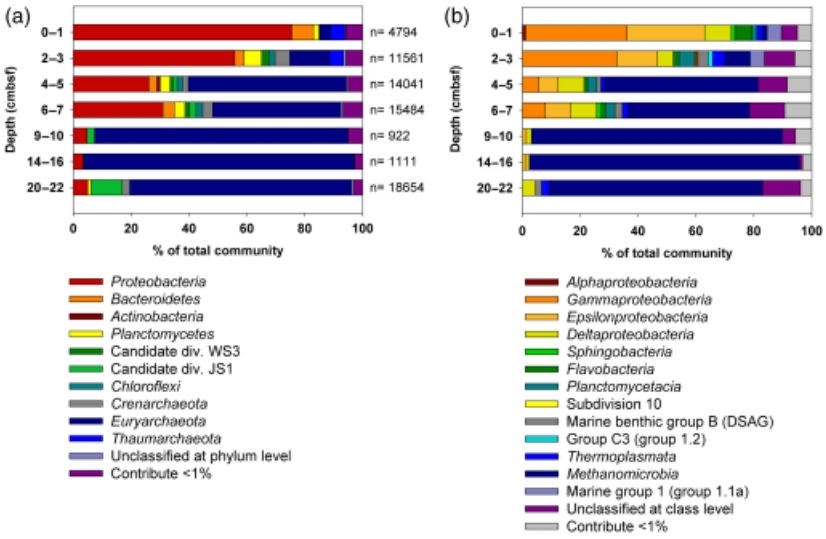

Fig. 2. Microbial community structure and abundance in core 29ROV. Taxonomical classification of 16S rRNA gene amplicons of archaeal and bacterial groups at phylum level (a) and class level (b). Groups that contribute $< 1\%$ to the total community are represented in the category: Contribute $< 1\%$. For each taxonomical level a quantum of the sequences remained unclassified due to the LCA algorithm in MEGAN. The column on the right side of (a) indicates the number of reads for each subsample retrieved by 454-pyrosequencing of the amplicons.

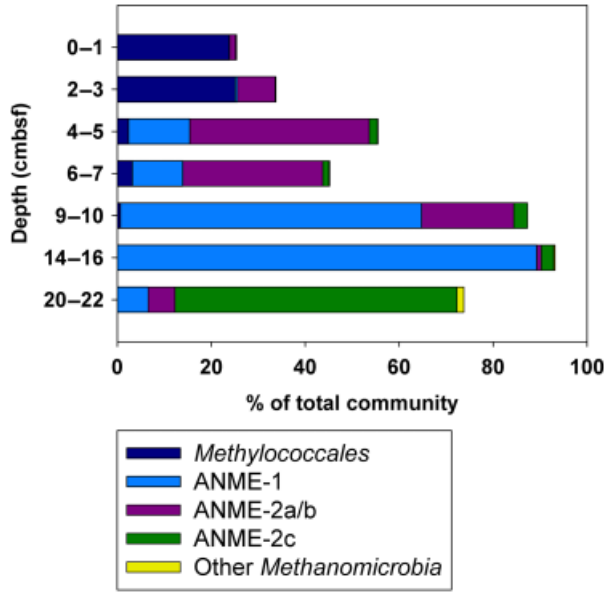

Fig. 3. Community structure of methanotrophs in core 29ROV. Abundance and stratification of aerobic methanotrophs within *Methylococcales* (*Gammaproteobacteria*) and anaerobic methanotrophs within ANME-subgroups (*Methanomicrobia*).

the hydrogen sulfide produced during AOM in deeper horizons (Lösekann *et al.*, 2007; Lloyd *et al.*, 2010). In sediment horizons from 0 to 3 cmbsf, the *Epsilonproteobacteria* were one of the most abundant taxa, comprising 26.8% and 14.1% of the total reads, respectively (Fig. 2b). More than 99% of these reads were assigned to members of the sulfur-oxidizing groups *Sulfurovum* and *Sulfurimonas*, of which *Sulfurovum* was the most dominant genus. Only minor fractions of *Epsilonproteobacteria* were observed in deeper horizons. Cultivated representatives of *Sulfurovum* and *Sulfurimonas* are described as chemolithoautotrophs oxidizing elemental sulfur, sulfide or thiosulfate coupled to reduction of oxygen or nitrate, and are abundant in hydrothermal vent systems (Inagaki *et al.*, 2003, 2004; Campbell *et al.*, 2006; Takai *et al.*, 2006; Glaubitz *et al.*, 2010). Furthermore, *Sulfurimonas* has been identified in the pelagic redoxcline of the Black Sea (Glaubitz *et al.*, 2010). However, in marine methane-enriched sediments, such as in the Gulf of Mexico, Håkon Mosby Mud Volcano and Hydrate Ridge, the sulfur-oxidizing bacteria *Beggiatoa* affiliated with *Gammaproteobacteria* form bacterial mats in the seawater-sediment interface (Sassen *et al.*, 1993; Knittel *et al.*, 2005; Lösekann *et al.*, 2007). The high abundance of *Epsilonproteobacteria* in the microbial mat in the G11 pockmark could indicate that the Nyegga area has a different geochemical composition or involves different environmental factors compared to other cold seep areas, and that these could influence the microbial colonization of the sediment surface located directly above seepage structures.

The dominating archaeal phylum in the two uppermost horizons was *Thaumarchaeota*, constituting 4.9% of the total community (Fig. 2). Within this phylum all sequences were affiliated with Marine Group 1.1a, of which cultivated representatives are described as aerobic autotrophic ammonia oxidizers (Könneke *et al.*, 2005; Walker *et al.*, 2010). In conclusion, the sediment horizons above 3 cmbsf were dominated by microorganisms involved in aerobic oxidative processes.

From 3 to 10 cmbsf, there was a gradual increase in abundance of other bacterial taxa within *Chloroflexi*, *Planctomycetes* and *Bacteroidetes*, contributing between 1.9% and

7.5% to the microbial communities (Fig. 2b). These taxa are often detected in marine sediments (Heijs *et al.*, 2007; Harrison *et al.*, 2009; Liao *et al.*, 2009); however, their ecological and metabolic role in these environments are not well studied. Remaining bacterial taxa constituting $< 1\%$ of the total reads are not described in detail (Appendix S1), although they contribute to the higher overall diversity of Bacteria compared with diversity of Archaea, especially in horizons above 10 cmbsf (Fig. S3).

The archaeal taxa *Thermoplasmata* within *Euryarchaeota* and Marine Benthic group B within *Crenarchaeota* were present mainly between 0 and 7 cmbsf, comprising 1.3–4.4%. Within *Thermoplasmata*, a majority of the reads were affiliated to Marine Benthic group D and the terrestrial miscellaneous euryarcheotal group, which are among the less abundant groups in marine sediments (Knittel *et al.*, 2005; Webster *et al.*, 2006). Marine Benthic group B, also known as deep-sea archaeal group (DSAG), might be involved in biochemical processes, including sulfate reduction or methane oxidation, based on increased presence of DSAG in the sulfate-reduction zone in hydrate-bearing sediments (Inagaki *et al.*, 2006).

Depth profile of ANME

Anaerobic methanotrophs (ANME), previously described as AOM-performing Archaea (Hinrichs *et al.*, 1999; Knittel & Boetius, 2009), dominated the Nyegga cold seep sediments below 4 cm (Fig. 3). In the oxic sediments surface horizons, dominated by sulfur-oxidizing bacteria and aerobic methanotrophs, only a few reads were assigned to ANME clades. The overall abundance of ANME increased with depth, and two of the major groups of ANME, ANME-1 and ANME-2, were identified. Transitions of ANME-2a/b-, ANME-1- and ANME-2c-dominated communities with increasing depth were observed, indicating distinct niche-specific stratification in this habitat (Fig. 3). Sulfide concentrations above 2.4 mM has been shown to inhibit AOM coupled to sulfate reduction (Meulepas *et al.*, 2009) in a mixed-culture with ANME-2a as the sole ANME (Jagersma *et al.*, 2009). The observed stratification of ANME may thus be caused by their ability to tolerate elevated sulfide concentrations and explain why ANME-2a/b was less abundant below 10 cmbsf. At 4–5 and 6–7 cmbsf, the ANME-2a/b subgroup comprised 38.1% and 29.8% of the total reads, respectively, whereas ANME-1 constituted $< 15\%$ in these layers. In the deepest layers (20–22 cmbsf), closest to the gas hydrates, the ANME-2c subgroup dominated the microbial community with 60% of the reads. The number of ANME-1 assigned reads increased with increasing sediment depth, and the highest abundance was observed at horizons 9–10 and 14–16 cmbsf, where 64.1% and 89.2% of the total reads were classified as ANME-1, respectively.

The qPCR results confirmed the predominance of Archaea in the horizons below 7–8 cmbsf (Fig. 1b), where the geochemical data implied AOM as a dominating process. The abundance of Archaea increased with increasing depth from 3.7×10^8 16S rRNA gene copies g^{-1} sediment at 7–8 cmbsf to a distinct peak in the ANME-1 dominated horizon at 14–16 cmbsf with 4.5×10^9 16S rRNA gene copies g^{-1} sediment. Overall, the total 16S rRNA gene copies enumerated by qPCR were in accordance with the relative numbers of Archaea and Bacteria in the amplicon dataset (Fig. 2 and Fig. S2), and also with other methane-enriched marine habitats such as the Black Sea (Leloup *et al.*, 2007) and the Haakon Mosby Mud Volcano (Lösekann *et al.*, 2007).

Between 33% and 98% of all ANME-1 affiliated reads throughout the sediment-core were not assigned to either ANME-1a or ANME-1b by the LCA algorithm in MEGAN. The ANME-1 sequences were thus extracted from MEGAN and subdivided into operational taxonomic units (OTUs) using the AMPLICONNOISE software and an in-house PERL script. The ANME-1 affiliated sequences were distributed in seven OTUs when a cut-off value of 0.03 was used (Table S2). The OTU-2 was present in all horizons and included 88.3% off all ANME-1 affiliated reads. A phylogenetic analysis based on one representative ANME-1 sequence from each OTU, and previously recovered ANME-1a/b sequences comprising a wide geographical distribution revealed that OTUs 1, 3, 4 and 5 were affiliated with ANME-1a whereas OTUs 2, 6 and 7 were classified as ANME-1b (Fig. S4). Hence, ANME-1b appears to dominate in the sediments within the pingo-structure in the G11 pockmark at Nyegga.

ANME and interspecies relations

ANME-1 and ANME-2 are most often associated with sulfate-reducing genera within *Desulfosarcina* and *Desulfococcus* (DSS) (*Deltaproteobacteria*), defined as SEEP-SRB-1 (Knittel & Boetius, 2009). Overall, reads classified as *Deltaproteobacteria* comprised 1.08–9.18% of the reads, of which the majority was assigned to known orders of sulfate reducers, such as *Desulfobacterales* and *Desulfuromonadales*. The abundance of the different families varied with increasing depth. Above the horizons enriched in ANME, *Desulfobulbaceae* dominated, of which *Desulfobulbus* and *Desulfocapsa* were the main genera. In the ANME-2a/b-dominated horizons, a predominance of *Desulfobacteraceae* was observed, and within this family the most abundant groups were *Desulfococcus*, described as a possible SRB partner of ANME during AOM (Boetius *et al.*, 2000; Knittel *et al.*, 2005; Schreiber *et al.*, 2010), and *Desulfobacterium*.

The ANME-1 dominated horizons had the lowest abundance of *Deltaproteobacteria*, contributing $< 2\%$ to the total community. All the bacterial reads were assigned to

Desulfobacterales, and the majorities were affiliated with *Desulfobacteraceae*. ANME-1 accounts for up to 33% of total single cells in sediments from Hydrate Ridge (Knittel *et al.*, 2005) and at least 70% of the microbial mat from the Black Sea (Michaelis *et al.*, 2002), and can form dense colonies of monospecific aggregates (Treude *et al.*, 2007). In order to provide further insight into the ANME-1 interspecies relationships, cells were extracted from the sediment at 14–16 cmbsf, and analyzed by FISH (Fig. 1c and d). Clearly, this horizon was dominated by ANME-1, occurring characteristically as single cells and in chains of two or more, where no direct contact with a bacterial partner was observed (Fig. 1d). The number of ANME-1 cells were approximately $2.54 \times 10^9\ g^{-1}$ sediment whereas Bacteria only constituted $9.93 \times 10^7\ g^{-1}$ sediment, in agreement with the qPCR results (Fig. 1b). Consequently, a highly abundant, naturally enriched ANME-1 community was present within the sediments at Nyegga.

Where ANME-2c was dominating, most of the reads within *Deltaproteobacteria* were assigned to *Desulfobacteraceae* at family level. ANME-2 has previously been observed with SRB in spherical shell-type or mixed type consortia (Boetius *et al.*, 2000; Orphan *et al.*, 2002; Knittel *et al.*, 2005). The ANME : SRB ratio in shell-type consortia has been found to be 1 : 3 in sediment samples from Hydrate Ridge (Orcutt & Meile, 2008). At Hydrate Ridge ANME-2/DSS aggregates accounted for $>$ 90% of the total cells, while single ANME-2 Archaea accounted for 1% (Knittel *et al.*, 2005). In the Nyegga sample, the *Deltaproteobacteria* were less abundant and calculated ratios of ANME/*Deltaproteobacteria* were as follows for the different horizons: 5.9 : 1 (4–5 cmbsf), 4.5 : 1 (6–7 cmbsf), 50 : 1 (9–10 cmbsf), 86 : 1 (14–16 cmbsf) and 16.1 : 1 (20–22 cmbsf). Monospecific aggregates of ANME-2 have previously been detected by FISH analyses of ANME communities in sediments from Eel River and Eckernförde Bay (Orphan *et al.*, 2002; Treude *et al.*, 2005), and microbial mats from the Black Sea (Treude *et al.*, 2007). The higher ratio of ANME/*Deltaproteobacteria* in the sediments at Nyegga could indicate that not all ANME-cells are aggregating with SRB, but may occur as single cells or in monospecific aggregates. Another interesting possibility is that ANME interspecies associations may extend beyond sulfate-reducing *Deltaproteobacteria* in the sediments at Nyegga, as observed for ANME-2c in Eel River sediments (Pernthaler *et al.*, 2008). In the Nyegga sediments, the bacterial group Candidate division Japan Sea 1 (JS-1) accounted for 1.4–10.8% of the reads. No cultivated representatives of JS-1 group exist, making physiological inferences impossible. However, the JS-1 group is widespread in deep marine subsurface sediments, and is associated with anaerobic organic-rich environments, methane hydrate containing sediments and anaerobic methanotrophic communities in sediments with high sulfate-reduction rates (Inagaki *et al.*, 2006; Webster *et al.*, 2007). To statistically analyze a possible correlation in abundance variations between ANME groups and JS-1, a Spearman rank order correlation test was used. The test revealed a correlation between ANME-2 and JS-1 with a *P*-value of 0.006 ($R^2 = 0.86$), indicating that JS-1 could be a potential syntrophic partner of ANME-2. In contrast, there was no correlation between ANME-1 and JS-1 (*P*-value = 0.6, $R^2 = 0.21$), showing that the abundances of these groups change with depth independent of each other.

Conclusion

There is a gradual transition of dominating taxa in the sediment below a white microbial mat sampled within an active pingo-structure in the G11 pockmark at Nyegga. In the microbial mat and shallow sediment horizons, aerobic methanotrophs within *Gammaproteobacteria* dominate, and are sustained by convection of methane to the sediment surface. Interestingly, another dominating taxon in these horizons is sulfur-oxidizing representatives within *Sulfurovum* (*Epsilonproteobacteria*), which is not frequently observed in cold seeps. Our geochemical data indicate AOM in the deepest horizons of the core, where sulfate is consumed and $\delta^{13}C_{DIC}$ is depleted. In horizons below 4 cmbsf, a stratification of ANME was observed in the order ANME-2a/b, ANME-1 and ANME-2c, which has previously not been described for cold seep sediments. As the concentrations of sulfide increases with depth, the observed stratification may reflect the sulfide tolerance of the different ANME subgroups, with ANME-2a/b being the most sensitive. The abundance of described sulfate-reducing partners within *Deltaproteobacteria* was low in ANME-dominated horizons. However, we hypothesize that Candidate division JS-1 could benefit from AOM or ANME-related metabolites as there was a clear correlation in abundance between JS-1 and ANME-2. Sediment horizons highly enriched in and dominated by free-living ANME-1 assemblages further challenge the theory of syntrophic AOM with sulfate.

Acknowledgements

This work was supported by the Norwegian Research Council (Project number 179560) and VISTA (Norwegian Academy of Science and Letters, and Statoil, project 6501). We acknowledge Captain John Hugo Johansen and the crew on the *R/V G.O. Sars* as well as the ROV pilots from ARGUS Remote Systems for all their support during the cruise to the Nyegga pockmark field in 2008. This paper is a contribution to the Norwegian Research Council PETROMAKS project 'Gas Hydrates on the Norwegian-Barents Sea-Svalbard Margin' (GANS, Norwegian Research Council project no. 175969/S30). Furthermore, we thank the Norwegian

Deepwater Program Seabed III for the financial support for collecting the cores. We acknowledge Katrin Knittel at MPI in Bremen, for guidance in the use of FISH and Frida Lise Daae at Department of Biology, Centre for Geobiology, University of Bergen for technical support.

References

Amann RI, Ludwig W & Schleifer KH (1995) Phylogenetic identification and *in situ* detection of individual microbial cells without cultivation. *Microbiol Rev* **59**: 143–169.

Boetius A, Ravenschlag K, Schubert CJ *et al.* (2000) A marine microbial consortium apparently mediating anaerobic oxidation of methane. *Nature* **407**: 623–626.

Brazelton WJ, Schrenk MO, Kelley DS & Baross JA (2006) Methane- and sulfur-metabolizing microbial communities dominate the Lost City hydrothermal field ecosystem. *Appl Environ Microb* **72**: 6257–6270.

Campbell BJ, Engel AS, Porter ML & Takai K (2006) The versatile epsilon-proteobacteria: key players in sulphidic habitats. *Nat Rev Microbiol* **4**: 458–468.

Chen Y, Ussler W III, Haflidason H, Lepland A, Rise L, Hovland M & Hjelstuen BO (2010) Sources of methane inferred from pore-water $\delta^{13}C$ of dissolved inorganic carbon in Pockmark G11, offshore Mid-Norway. *Chem Geol* **275**: 127–138.

Christensen H, Hansen M & Sorensen J (1999) Counting and size classification of active soil bacteria by fluorescence *in situ* hybridization with an rRNA oligonucleotide probe. *Appl Environ Microb* **65**: 1753–1761.

Daims HBA, Amann R, Schleifer KH & Wagner M (1999) The domain-specific probe EUB338 is insufficient for the detection of all Bacteria: development and evaluation of a more comprehensive probe set. *Syst Appl Microbiol* **22**: 434–444.

Edwards U, Rogall T, Blocker H, Emde M & Bottger EC (1989) Isolation and direct complete nucleotide determination of entire genes. Characterization of a gene coding for 16S ribosomal RNA. *Nucleic Acids Res* **17**: 7843–7853.

Einen J, Thorseth IH & Ovreas L (2008) Enumeration of Archaea and Bacteria in seafloor basalt using real-time quantitative PCR and fluorescence microscopy. *FEMS Microbiol Lett* **282**: 182–187.

Fang J, Shizuka A, Kato C & Schouten S (2006) Microbial diversity of cold-seep sediments in Sagami Bay, Japan, as determined by 16S rRNA gene and lipid analyses. *FEMS Microbiol Ecol* **57**: 429–441.

Glaubitz S, Labrenz M, Jost G & Jurgens K (2010) Diversity of active chemolithoautotrophic prokaryotes in the sulfidic zone of a Black Sea pelagic redoxcline as determined by rRNA-based stable isotope probing. *FEMS Microbiol Ecol* **74**: 32–41.

Glöckner FO, Amann R, Alfreider A, Pernthaler J, Psenner R, Trebesius K & Schleifer KH (1996) An *in situ* hybridization protocol for detection and identification of planktonic bacteria. *Syst Appl Microbiol* **19**: 403–406.

Harrison BK, Zhang H, Berelson W & Orphan VJ (2009) Variations in archaeal and bacterial diversity associated with the sulfate-methane transition zone in continental margin sediments (Santa Barbara Basin, California). *Appl Environ Microb* **75**: 1487–1499.

Heijs SK, Haese RR, van der Wielen PW, Forney LJ & van Elsas JD (2007) Use of 16S rRNA gene based clone libraries to assess microbial communities potentially involved in anaerobic methane oxidation in a Mediterranean cold seep. *Microb Ecol* **53**: 384–398.

Hinrichs KU, Hayes JM, Sylva SP, Brewer PG & DeLong EF (1999) Methane-consuming archaebacteria in marine sediments. *Nature* **398**: 802–805.

Hjelstuen BO, Haflidason H, Sejrup HP & Nygard A (2010) Sedimentary and structural control on pockmark development-evidence from the Nyegga pockmark field, NW European margin. *Geo-Mar Lett* **30**: 221–230.

Hoehler TM, Alperin MJ, Albert DB & Martens CS (1994) Field and laboratory studies of methane oxidation in an anoxic marine sediment – evidence for a methanogen-sulfate reducer consortium. *Global Biogeochem Cy* **8**: 451–463.

Hovland M, Svensen H, Forsberg CF, Johansen H, Fichler C, Fossa JH, Jonsson R & Rueslatten H (2005) Complex pockmarks with carbonate-ridges off mid-Norway: Products of sediment degassing. *Mar Geol* **218**: 191–206.

Hugler M, Gartner A & Imhoff JF (2010) Functional genes as markers for sulfur cycling and CO_2 fixation in microbial communities of hydrothermal vents of the Logatchev field. *FEMS Microbiol Ecol* **73**: 526–537.

Huson DH, Auch AF, Qi J & Schuster SC (2007) MEGAN analysis of metagenomic data. *Genome Res* **17**: 377–386.

Inagaki F, Takai K, Kobayashi H, Nealson KH & Horikoshi K (2003) *Sulfurimonas autotrophica* gen. nov., sp. nov., a novel sulfur-oxidizing epsilon-proteobacterium isolated from hydrothermal sediments in the Mid-Okinawa Trough. *Int J Syst Evol Micr* **53**: 1801–1805.

Inagaki F, Takai K, Nealson KH & Horikoshi K (2004) *Sulfurovum lithotrophicum* gen. nov., sp. nov., a novel sulfur-oxidizing chemolithoautotroph within the epsilon-Proteobacteria isolated from Okinawa Trough hydrothermal sediments. *Int J Syst Evol Micr* **54**: 1477–1482.

Inagaki F, Nunoura T, Nakagawa S *et al.* (2006) Biogeographical distribution and diversity of microbes in methane hydrate-bearing deep marine sediments on the Pacific Ocean Margin. *P Natl Acad Sci USA* **103**: 2815–2820.

Ivanov M, Mazzini A, Blinova V, Kozlova E, Laberg JS, Matveeva T, Taviani M & Kaskov N (2010) Seep mounds on the Southern Wiring Plateau (offshore Norway). *Mar Petrol Geol* **27**: 1235–1261.

Jagersma GC, Meulepas RJ, Heikamp-de Jong I, Gieteling J, Klimiuk A, Schouten S, Damste JS, Lens PN & Stams AJ (2009) Microbial diversity and community structure of a highly active anaerobic methane-oxidizing sulfate-reducing enrichment. *Environ Microbiol* **11**: 3223–3232.

Knittel K & Boetius A (2009) Anaerobic oxidation of methane: progress with an unknown process. *Annu Rev Microbiol* **63**: 311–334.

Knittel K, Lösekann T, Boetius A, Kort R & Amann R (2005) Diversity and distribution of methanotrophic archaea at cold seeps. *Appl Environ Microb* **71**: 467–479.

Könneke M, Bernhard AE, de la Torre JR, Walker CB, Waterbury JB & Stahl DA (2005) Isolation of an autotrophic ammonia-oxidizing marine archaeon. *Nature* **437**: 543–546.

Kvenvolden KA, Ginsburg GD & Soloviev VA (1993) Worldwide distribution of subaquatic gas hydrates. *Geo-Mar Lett* **13**: 32–40.

Lane DJ (1991) 16S/23S rRNA sequencing. *Nucleic Acid Techniques in Bacterial Systematics* (Stackebrandt E & Goodfellow M, eds), pp. 115–175. Wiley, New York, NY.

Lane DJ, Pace B, Olsen GJ, Stahl DA, Sogin ML & Pace NR (1985) Rapid determination of 16S ribosomal RNA sequences for phylogenetic analyses. *P Natl Acad Sci USA* **82**: 6955–6959.

Lanoil BD, Sassen R, La Duc MT, Sweet ST & Nealson KH (2001) Bacteria and Archaea physically associated with Gulf of Mexico gas hydrates. *Appl Environ Microb* **67**: 5143–5153.

Lanzen A, Jorgensen SL, Bengtsson MM, Jonassen I, Overas L & Urich T (2011) Exploring the composition and diversity of microbial communities at the Jan Mayen hydrothermal vent field using RNA and DNA. *FEMS Microbiol Ecol* doi: 10.1111/j.1574-6941.2011.01138.x.

Leloup J, Loy A, Knab NJ, Borowski C, Wagner M & Jorgensen BB (2007) Diversity and abundance of sulfate-reducing microorganisms in the sulfate and methane zones of a marine sediment, Black Sea. *Environ Microbiol* **9**: 131–142.

Liao L, Xu XW, Wang CS, Zhang DS & Wu M (2009) Bacterial and archaeal communities in the surface sediment from the northern slope of the South China Sea. *J Zhejiang Univ Sci B* **10**: 890–901.

Lloyd KG, Lapham L & Teske A (2006) An anaerobic methane-oxidizing community of ANME-1b archaea in hypersaline Gulf of Mexico sediments. *Appl Environ Microb* **72**: 7218–7230.

Lloyd KG, Albert DB, Biddle JF, Chanton JP, Pizarro O & Teske A (2010) Spatial structure and activity of sedimentary microbial communities underlying a *Beggiatoa* spp. mat in a Gulf of Mexico hydrocarbon seep. *PLoS One* **5**: e8738.

Lösekann T, Knittel K, Nadalig T, Fuchs B, Niemann H, Boetius A & Amann R (2007) Diversity and abundance of aerobic and anaerobic methane oxidizers at the Haakon Mosby Mud Volcano, Barents Sea. *Appl Environ Microb* **73**: 3348–3362.

Loy A, Lehner A, Lee N, Adamczyk J, Meier H, Ernst J, Schleifer K-H & Wagner M (2002) Oligonucleotide microarray for 16S rRNA gene-based detection of all recognized lineages of sulfate-reducing prokaryotes in the environment. *Appl Environ Microb* **68**: 5064–5081.

Meulepas RJ, Jagersma CG, Khadem AF, Buisman CJ, Stams AJ & Lens PN (2009) Effect of environmental conditions on sulfate reduction with methane as electron donor by an Eckemforde Bay enrichment. *Environ Sci Technol* **43**: 6553–6559.

Michaelis W, Seifert R, Nauhaus K *et al.* (2002) Microbial reefs in the Black Sea fueled by anaerobic oxidation of methane. *Science* **297**: 1013–1015.

Morikawa K & Yanagida M (1981) Visualization of Individual DNA Molecules in Solution by Light Microscopy: DAPI Staining Method. *J Biochem* **89**: 693–696.

Muyzer G, de Waal EC & Uitterlinden AG (1993) Profiling of complex microbial populations by denaturing gradient gel electrophoresis analysis of polymerase chain reaction-amplified genes coding for 16S rRNA. *Appl Environ Microb* **59**: 695–700.

Muyzer G, Teske A, Wirsen CO & Jannasch HW (1995) Phylogenetic relationships of *Thiomicrospira* species and their identification in deep-sea hydrothermal vent samples by denaturing gradient gel electrophoresis of 16S rDNA fragments. *Arch Microbiol* **164**: 165–172.

Nauhaus K, Boetius A, Kruger M & Widdel F (2002) *In vitro* demonstration of anaerobic oxidation of methane coupled to sulphate reduction in sediment from a marine gas hydrate area. *Environ Microbiol* **4**: 296–305.

Niemann H, Lösekann T, de Beer D *et al.* (2006) Novel microbial communities of the Haakon Mosby mud volcano and their role as a methane sink. *Nature* **443**: 854–858.

Orcutt B & Meile C (2008) Constraints on mechanisms and rates of anaerobic oxidation of methane by microbial consortia: process-based modeling of ANME-2 archaea and sulfate reducing bacteria interactions. *Biogeosciences* **5**: 1587–1599.

Orphan VJ, Hinrichs KU, Ussler W III, Paull CK, Taylor LT, Sylva SP, Hayes JM & Delong EF (2001) Comparative analysis of methane-oxidizing archaea and sulfate-reducing bacteria in anoxic marine sediments. *Appl Environ Microb* **67**: 1922–1934.

Orphan VJ, House CH, Hinrichs KU, McKeegan KD & DeLong EF (2002) Multiple archaeal groups mediate methane oxidation in anoxic cold seep sediments. *P Natl Acad Sci USA* **99**: 7663–7668.

Ovreas L, Forney L, Daae FL & Torsvik V (1997) Distribution of bacterioplankton in meromictic Lake Saelenvannet, as determined by denaturing gradient gel electrophoresis of PCR-amplified gene fragments coding for 16S rRNA. *Appl Environ Microb* **63**: 3367–3373.

Pachiadaki MG, Lykousis V, Stefanou EG & Kormas KA (2010) Prokaryotic community structure and diversity in the sediments of an active submarine mud volcano (Kazan mud volcano, East Mediterranean Sea). *FEMS Microbiol Ecol* **72**: 429–444.

Pernthaler A, Dekas AE, Brown CT, Goffredi SK, Embaye T & Orphan VJ (2008) Diverse syntrophic partnerships from deep-sea methane vents revealed by direct cell capture and metagenomics. *P Natl Acad Sci USA* **105**: 7052–7057.

Quince C, Lanzen A, Davenport RJ & Turnbaugh PJ (2011) Removing noise from pyrosequenced amplicons. *BMC Bioinformatics* **12**: 38.

Reeburgh WS (2007) Oceanic methane biogeochemistry. *Chem Rev* **107**: 486–513.

Reiche S, Hjelstuen BO & Haflidason H (2011) High-resolution seismic stratigraphy, sedimentary processes and the origin of seabed cracks and pockmarks at Nyegga, mid-Norwegian margin. *Mar Geol* **284**: 28–39.

Roesch LF, Fulthorpe RR, Riva A *et al.* (2007) Pyrosequencing enumerates and contrasts soil microbial diversity. *ISME J* **1**: 283–290.

Ronimus RS, Reysenbach A, Musgrave DR & Morgan HW (1997) The phylogenetic position of the *Thermococcus* isolate AN1 based on 16S rRNA gene sequence analysis: a proposal that AN1 represents a new species, *Thermococcus zilligii* sp. nov. *Arch Microbiol* **168**: 245–248.

Sassen R, Roberts HH, Aharon P, Larkin J, Chinn EW & Carney R (1993) Chemosynthetic bacterial mats at cold hydrocarbon seeps, Gulf of Mexico continental-slope. *Org Geochem* **20**: 77–89.

Schreiber L, Holler T, Knittel K, Meyerdierks A & Amann R (2010) Identification of the dominant sulfate-reducing bacterial partner of anaerobic methanotrophs of the ANME-2 clade. *Environ Microbiol* **12**: 2327–2340.

Steinsbu BO, Thorseth IH, Nakagawa S, Inagaki F, Lever MA, Engelen B, Ovreas L & Pedersen RB (2010) *Archaeoglobus sulfaticallidus* sp. nov., a novel thermophilic and facultatively lithoautotrophic sulfate-reducer isolated from black rust exposed to hot ridge flank crustal fluids. *Int J Syst Evol Micr* **1**: 1–2.

Stoecker K, Dorninger C, Daims H & Wagner M (2010) Double labeling of oligonucleotide probes for fluorescence *in situ* hybridization (DOPE-FISH) improves signal intensity and increases rRNA accessibility. *Appl Environ Microb* **76**: 922–926.

Takai K, Suzuki M, Nakagawa S, Miyazaki M, Suzuki Y, Inagaki F & Horikoshi K (2006) *Sulfurimonas paralvinellae* sp. nov., a novel mesophilic, hydrogen- and sulfur-oxidizing chemolithoautotroph within the Epsilonproteobacteria isolated from a deep-sea hydrothermal vent polychaete nest, reclassification of *Thiomicrospira denitrificans* as *Sulfurimonas denitrificans* comb. nov. and emended description of the genus *Sulfurimonas*. *Int J Syst Evol Micr* **56**: 1725–1733.

Treude T, Kruger M, Boetius A & Jorgensen BB (2005) Environmental control on anaerobic oxidation of methane in the gassy sediments of Eckernforde Bay (German Baltic). *Limnol Oceanogr* **50**: 1771–1786.

Treude T, Orphan V, Knittel K, Gieseke A, House CH & Boetius A (2007) Consumption of methane and CO_2 by methanotrophic microbial mats from gas seeps of the anoxic Black Sea. *Appl Environ Microb* **73**: 2271–2283.

Treusch AH, Leininger S, Kletzin A, Schuster SC, Klenk HP & Schleper C (2005) Novel genes for nitrite reductase and Amo-related proteins indicate a role of uncultivated mesophilic crenarchaeota in nitrogen cycling. *Environ Microbiol* **7**: 1985–1995.

Walker CB, de la Torre JR, Klotz MG *et al.* (2010) *Nitrosopumilus maritimus* genome reveals unique mechanisms for nitrification and autotrophy in globally distributed marine crenarchaea. *P Natl Acad Sci USA* **107**: 8818–8823.

Webster G, Parkes RJ, Cragg BA, Newberry CJ, Weightman AJ & Fry JC (2006) Prokaryotic community composition and biogeochemical processes in deep subseafloor sediments from the Peru Margin. *FEMS Microbiol Ecol* **58**: 65–85.

Webster G, Yarram L, Freese E, Koster J, Sass H, Parkes RJ & Weightman AJ (2007) Distribution of candidate division JS1 and other Bacteria in tidal sediments of the German Wadden Sea using targeted 16S rRNA gene PCR-DGGE. *FEMS Microbiol Ecol* **62**: 78–89.

Wegener G, Shovitri M, Knittel K, Niemann H, Hovland M & Boetius A (2008) Biogeochemical processes and microbial diversity of the Gullfaks and Tommeliten methane seeps (Northern North Sea). *Biogeosciences* **5**: 1127–1144.

Whelan JA, Russell NB & Whelan MA (2003) A method for the absolute quantification of cDNA using real-time PCR. *J Immunol Methods* **278**: 261–269.

Zipper H, Buta C, Lammle K, Brunner H, Bernhagen J & Vitzthum F (2003) Mechanisms underlying the impact of humic acids on DNA quantification by SYBR Green I and consequences for the analysis of soils and aquatic sediments. *Nucleic Acids Res* **31**: e39.

Supporting Information

Additional Supporting Information may be found in the online version of this article:

Table S1. Reads from 454 pyrosequencing filtered by PyroNoise.
Table S2. Percent wise distribution of ANME-1 reads in OTUs.
Figure S1. Photos of the sampling site inside the G11 pockmark at Nyegga (a), and the core 29ROV used in this study (b).
Figure S2. Variation in abundance of Archaea quantified by both qPCR and amplicons in horizons throughout the core, shown as percent of total reads or archaeal and bacterial cells summarized, respectively.
Figure S3. Rarefaction curves of Archaea (a) and Bacteria (b).
Figure S4. Phylogenetic tree showing the affiliations of OTU representatives of ANME-1 16S rRNA gene sequences from Nyegga sediments and selected archael reference sequences.
Appendix S1. An overview of the taxonomic binning of all reads from each subsample.

Please note: Wiley-Blackwell is not responsible for the content or functionality of any supporting materials supplied by the authors. Any queries (other than missing material) should be directed to the corresponding author for the article.